Comparison of complexed species of Eu in alumina-bound and free polyacrylic acid: A spectroscopic study

Gilles Montavon, C. Hennig, P. Janvier, Bernd Grambow

Comparison of complexed species of Eu in Alumina-bound and free Polyacrylic Acid. A spectroscopic study.

G. Montavon[*], C. Hennig[⊥], P. Janvier [°] and B. Grambow

Laboratoire SUBATECH, 4 rue A. Kastler, BP 20722, 44307 Nantes cedex 03, France

[⊥] *Forschungszentrum Rossendorf, Institute of Radiochemistry, P.O. Box 510119, 01314 Dresden, Germany*

[°] *LSO, 2 rue de la Houssinière - BP 92208 - 44322 NANTES Cedex 3*

[*]corresponding author; phone: 33(0)251858420; fax: 33(0)251858452; e-mail: montavon@subatech.in2p3.fr.

Abstract

The speciation of Eu complexed with polyacrylic acid (PAA) and alumina-bound PAA (PAA_{ads}) was studied at pH=5 in 0.1M $NaClO_4$. Structural parameters were obtained from $^7F_0 \rightarrow {}^5D_0$ excitation spectra measured by Laser Induced Fluoresence Spectroscopy as well as from Eu L_{III} edge Extended X-ray Absorption Fine Structure (EXAFS) spectra. The coordination mode was also investigated by infrared spectroscopy. To elucidate the nature of the complexed species, Eu-acetate complexes were used as references. The spectroscopic techniques show that two carboxylate groups with 2-3 (EuPAA) and 4-5 ($EuPAA_{ads}$) water molecules are coordinated to Eu in the first coordination sphere. For $EuPAA_{ads}$, the coordination between carboxylate groups and Eu appears to be bidendate. A similar coordination is probable for EuPAA but the EXAFS data indicate a sligthly distorted coordination. The results show that the degree of freedom of carboxylate groups is not the same for free or adsorbed PAA. For PAA, the degree of freedom is constrained by the flexibility of the methylene chain. When PAA is adsorbed on alumina, the polymer chains cannot any more be treated as independent chains. One may rather assume formation of aggregates that form an organic layer at the mineral surface presenting a complex arrangement of carboxylate groups.

Keywords: polyacrylic acid; Eu; LIFS, FTIR, EXAFS; speciation; adsorption; ternary system

Introduction

For the assessment of radionuclide mobility in contaminated soils, the interaction between actinide metal ions, M, and humic substances, HS, has been the subject of various studies [1-3]. These studies have been carried out notably with trivalent actinides (Cm, Am) and chemical homologues (e.g. Eu), as their solution behavior in the environment under given conditions is known to be dominated by organic macromolecules [1]. The interaction depends on the chemical state of the organic material, which can be soluble or associated to mineral particles. Numerous studies on the interaction of actinides with HS in solution are described in the literature [1-4], but few studies have been devoted to the interaction of actinides with HS-mineral complexes [5-13].

In most cases, the metal ion interaction with the organic-mineral complex can not be described simply by combining the behavior observed in the individual binary systems M/HS and M/mineral phase [14]. To understand the M/HS-mineral interactions, simplified systems are used. Polycarboxylic acids [15-18] were selected as model systems allowing to study the role of the polyelectrolyte character and of carboxylic groups in the interaction. In a recent study using polyacrylic acid (PAA) [17], the interaction of M(III) (M=Cm,Eu) with mineral-adsorbed PAA appeared different from the interaction with dissolved PAA. The M(III)/PAA interaction can be described by considering PAA as a classical organic ligand [19]. The interaction between M(III) and PAA_{ads} is more complex: after a rapid attachment of M(III) at the organic-mineral surface, a modification of M(III) speciation occurs. The origin of this discrepancy may be explained by the difference in PAA configuration in the two systems.

To get further insight into the difference between the complexation behaviour of sorbed and free polyelectrolytes, both systems are compared in this study using spectroscopic methods. As described previously [18], the ternary system is composed of γ-alumina, Eu and a

polycarboxylic acid. Experimental conditions were chosen to selectively study the interaction between Eu and adsorbed PAA in the ternary system, i.e. without considering the interaction of Eu with aluminol surface sites [7].

The speciation of Eu (total coordination number, number of carboxylate groups and water molecules bound, distances, coordination mode) was characterized in this study using $^7F_0 \rightarrow {}^5D_0$ excitation spectra [20,21] measured by Laser Induced Fluorescence Spectroscopy (LIFS) as well as by Eu L_{III} edge Extended X-ray Absorption Fine Structure (EXAFS) spectra. The coordination mode was also assessed for the EuPAA complex by infrared (IR) spectroscopy. To elucidate the nature of the complexed species in binary EuPAA and ternary $EuPAA_{ads}$ systems, Eu / acetate (Ac) system was used as reference.

Materials and Methods

(A) Chemicals. Commercially available sodium perchlorate monohydrate (Fluka, purum), Europium oxide (Prolabo, RECTAPUR^{TM}), sodium acetate RP (Prolabo), cellulose 20µm, Eu triacetate, potassium bromide 99%, and polyacrylic acid at 5000Da (Aldrich) were used as received. The proton exchange capacity of PAA amounts to 11.3±0.4 meq/g [19]. γ-alumina was purchased from Degussa - Huls (aluminium oxide C, primary particle size of 20 nm, specific surface area of $100 m^2/g$, site density of $1 nm^{-2}$ [22]) and was used without further purification.

(B) Experimental Procedures. All solutions were prepared using Milli-Q water and all experiments were conducted in polyethylene tubes at room temperature under atmospheric conditions.

The preparing method of alumina-bound polyacrylic acid colloids is given in [18]. The concentration in the stock suspensions, c, expressed in terms of alumina concentration (in

g/L), was determined by drying at 105°C. The degree of PAA loading, corresponding to the ratio between concentrations of sorbed PAA (in mg/L) and of alumina (in g/L), was equal to Γ=59±3 mg/g. This value corresponds to the maximum of adsorption deduced from isotherm data [23]. Under these conditions, the alumina surface is saturated by PAA. No significant desorption of the initially adsorbed PAA occurred (i.e. below 6%) neither during the preparation of the stock suspension nor in the experiments with Eu.

(C) Sample preparation. The sample is characterized by the ligand-to-metal ratio defined as:

$$r = \frac{[COOH]_{tot}}{[EuPAA(ads)]} \quad (1)$$

with $[COOH]_{tot}$ and $[EuPAA_{(ads)}]$ being the total concentration (in mol/L) of carboxylic groups and the concentration of Eu complexed with either PAA or PAA_{ads}, respectively. To allow to compare the complexation properties with respect to Eu of free and of sorbed PAA, the experimental conditions were chosen in the ternary system in a way that the interaction of Eu with aluminol surface sites could be neglected: all experiments were carried out at pH=5 in 0.1 M $NaClO_4$ [7] with the alumina surface saturated by PAA. A list of the samples used in the study and the experimental conditions are given in Table 1. The experiments performed can be divided into three series:

- The first series includes the reference compounds (Eu/Ac system); conditions are chosen to get the spectroscopic characteristics of 1:1, 1:2 and 1:3 Eu:Ac complexes. Hydrated solids as well as solutions are used.
- The second series, consisting of a single sample, is linked to the binary EuPAA system. Conditions are chosen where EuPAA precipitates. The total Eu concentration was sufficient for EXAFS measurements and the speciation is representative to soluble EuPAA complex for a wide range of r values (r<300) [19].

- The third series comprises samples prepared to study the ternary $EuPAA_{ads}$ system. Conditions are chosen to assess the effect of r and the nature the samples (hydrated solids and suspension) on the speciation.

For preparing reference solution samples, Eu was mixed with the desired acetate concentration. The pH value was adjusted to 6. For EuPAA and $EuPAA_{ads}$ complexes, Eu was mixed at pH=5 in 0.1M $NaClO_4$ before the addition of PAA or PAA_{ads}. The contact time was at least 1 week [18]. To prepare the hydrated solids, the colloidal phase (EuPAA (precipitate) or $EuPAA_{ads}$) was separated from the solution by centrifugation for 15 minutes at 36000g. The obtained solid was then air-dried before spectroscopic measurements.

For LIFS measurements, hydrated solids as well as suspensions were analysed in quartz capillaries. For EXAFS and IR measurements, pellets (100mg) of 1.25 cm in diameter were prepared. Cellulose (EXAFS) and anhydrous KBr (IR) were used as a supporting material in a 1:1 weight ratio. For EXAFS measurements, the pellets were encapsulated in Kapton foils.

(D)Analytical Methods. A PQ-Excel ICP-MS (VG-Elemental) was used to analyse Eu concentration for r determination. The PAA concentration was analyzed by Total Organic Carbon (TOC) measurements using a Shimadzu TOC 5000A analyzer. IR spectra were recorded on a IR-TF Vector 22 Brüker.

(E) LIFS. All fluorescence experiments were carried out at room temperature at the Nuclear Physics Institute (Orsay University, France). The characteristics of the instrumental design can be found elsewhere [24]. The excitation wavelength was varied from 578 to 580 with an interval of 0.05nm. The excitation spectra were determined by integration, for a given excitation wavelength, of fluorescence intensity of the emission peak at 616nm. A minimum of two to three spectra were acquired and averaged for each sample. The deconvolution of the

excitation spectra was performed considering that peak(s) can be described by Lorentzian and Gaussian contributions [25] given by:

$$y = I\frac{\exp(-0.5*(\frac{x-w}{L})^2)}{(\frac{x-w}{L})^2+1} \qquad (2)$$

where I, w and L are the intensity, peak position, and linewidth, repectively. All fittings were performed with the SigmaPlot software using the Marquardt-Levenberg algorithm (version 2.0, Jandel Co.). Uncertainties associated to the fitting parameters were determined by the software.

(F) EXAFS. Europium L_{III}-edge X-ray absorption spectra at 6976.9 eV were recorded at room temperature at the Rossendorf Beamline (ROBL) [26], ERSF Grenoble, in fluorescence ($EuPAA_{ads}$) or transmission ($EuAc_3.xH_20$ and EuPAA) modes. For the fluorescence measurements, a 4-pixel Ge solid state detector was used. The monochromator was equipped with a Si(111) double-crystal. For each sample, at least 3 scans were collected. Addition and normalisation of X-ray absorption spectra, extraction of EXAFS oscillations and data analysis were performed with the EXAFSPAK program [27]. The EXAFS oscillations were isolated from the raw, averaged data by removal of the pre-edge background, approximated by a first-order polynomial. The extracted EXAFS spectra, obtained via spline fitting techniques and normalized using a Victoreen function, were Fourier-transformed using the k range 1.5-11.5 $Å^{-1}$ (except for the theoretical spectrum where the k range was extended to 14 $Å^{-1}$). The k range is limited by the occurrence of L_{II}-edge X-ray absorption at 7617.1 eV.

The curve-fitting analysis was carried out using the EXAFS equation [27] with the amplitude reduction factor S_0^2 set to 1. The theoretical scattering phases and amplitudes used in data analysis were calculated with the scattering code FEFF8 [28] using the crystal structure of $[Eu(\mu\text{-}CH_3COO\text{-}O)(CH_3COO)_2(H_2O)_2]_2.4H_2O$ [29]. The input file for FEFF8 was obtained

from ATOMS 3.0 program [30] considering the cluster presented in Figure 1. Errors associated to the fit procedure are ±20% for the coordination numbers and ±0.02Å for absorber-backscatterer distances.

Results and discussion

(A) LIFS study. Excitation spectra measured for the reference Eu / acetate system are presented in Figure 2. Four different species can be determined by deconvolution of excitation spectra. They are characterized by peak positions at 578.8, 579, 579.3 and 579.6nm. With respect to the composition of the samples (Table 1), peak positions at 579, 579.3 and 579.6nm characterize 1:1, 1:2 and 1:3 Eu:Ac complexes, respectively. The values are in accordance with the work of Yoon et al. [31] (579.04, 579.27 and 579.55 nm for 1:1, 1:2 and 1:3 complexes, respectively) but desagree with the one of Choppin & Wang [21] et al. (578.93, 579 and 579.2 nm for 1:1, 1:2 and 1:3 complexes, respectively). A slight shift of the peak position and a difference in linewith are observed for 1:3 complex between solid and liquid samples. In the solid sample $Eu.Ac_3.xH_2O$, a slight contamination with a 1:2 complex Eu:Ac is evidenced.

Concerning the fourth species, it must be associated to free Eu, in agreement with solution speciation (Table 1),. This appears coherent with the value of 578.83 nm reported for the aqueous species of Eu in [21]. The spectrum is characterized by a linewith (0.8 nm) which is higher than for the acetate complexes (0.4-0.5 nm).

Figure 3A presents the excitation spectra obtained for the ternary system with suspensions as a function of different ligand-to-metal ratios r. No significant effect is observed with r variation. Excitation spectra can be described by the presence of one complexed species characterized by a peak position of 578.17 nm and a linewith of 0.4 nm (see Table 1). Figures 3B and 3C give excitation spectra of $EuPAA_{ads}$ complexes conditionned in the solid state. The

excitation spectrum obtained at r=3330 corresponds to that measured for the same ligand-to-metal ratio in suspension. For the hydrated solid with r=33 (Figure 3C), the appearance of a small amount of another species is oberved. The peak position and the high linewidth indicate the presence of free Eu. Finally, Figure 3D gives the excitation spectra obtained for EuPAA complex. It coincides with that measured for $EuPAA_{ads}$ in the solid state at r=33 (see Table 1). The presence of Eu in both $EuPAA_{ads}$ and EuPAA samples may be the result of a slight contamination with non-complexed Eu.

In conclusion, a similar coordination configuration in binary and ternary systems is found irrespective of the r value. It appears that the drying step to pass from the suspension to the hydrated solid has no effect on Eu speciation. By comparison with the reference system, a 1:2 $Eu:COO^-$ coordination is expected in both EuPAA and $EuPAA_{ads}$ complexes. This 1:2 coordination was already proposed for soluble EuPAA complex (r=18) [31].

(B) IR study. For a sensitivity reason , IR spectra were recorded only for the $EuAc_3$ and EuPAA complexes. The spectra are presented in Figure 4. According to the literature, Δ values $[\nu_a(CO_2^-)-\nu_s(CO_2^-)]$ give an indication on the coordination mode between metal ions and carboxylate groups [32]. Based on the examination of many IR spectra of many acetate compounds with known X-ray crystal structures, the authors [32] came to the conclusion that Δ values around 164-228 and 42-77 cm^{-1} indicate monodentate and bidendate modes of coordination, respectively.

The analyse of IR spectra measured for hydrated solids give Δ values of 88 and 65 for $EuAc_3$ and EuPAA complexes, respectively. This indicates the existence of a bidendate mode of coordination for both systems.

Based on IR and LIFS measurements, 4 oxygen atoms of two acetate groups are coordinated in a bidendate fashion to Eu in EuPAA and $EuPAA_{ads}$ complexes. Considering a total

coordination number of 8-9 aroud Eu [33], the remaining 4-5 oxygen atoms can be attributed to water molecules.

(C) X-ray absorption experiments.

Theoretical considerations: The calculated EXAFS and the corresponding Fourier Transform (FT) (k range =1-14 $Å^{-1}$) spectra are given in Figure 5A-B (dotted lines) for the simple cluster, i.e. with one Eu coordinated to 3 carboxylate groups and three water molecules. The FT displays three main peaks, which can be described in a simplified manner as follows:

- The first FT peak at R+ΔR value of 2 Å arises from the single scaterring (SS) of the photoelectron on oxygen atoms in the first coordination sphere. The distance difference between Eu and O belonging to water molecules ($O(H_2)$, mean value of 2.39 Å) and carboxylate groups (O(Ac), mean value of 2.49 Å) is not large enough to allow an unambiguous distinction in peak analysis (the resolution limit for k = 1-14 $Å^{-1}$ is 0.12Å). The peak presents also a small contribution where carbon atoms C3, C5 and C1 (Figure 1) in the second shell act as backscatterers.
- The second (weak) peak at R+ΔR value of 2.7 Å results from the twofold degenerated 3-legged multiple scaterring (MS) path Eu-C(1,3,5)-O(Ac) (scattering path 4 in Table 2).
- The third peak at R+ΔR value of 4 Å arises from SS and 3,4-legged MS paths considering Eu C(1,3,5) and C(2,4,6) atoms (scattering paths 5-7 in Table 2). These complex backscattering features result from the linear arrangement of Eu and the two carbon atoms C1 (3 or 5) and C2 (4 or 6). In such a case, the scattering amplitude is greatly enhanced in the forward scattering direction due to focusing the electron wave to the next neighbor ("focusing effect"). This peak appears as the main signature of the bidendate mode of coordination. It appears possible to determine the distribution

$O(H_2)$/O(AC) in the first oxygen shell using these contributions, i.e. the number of carbon atoms fitted based on the third peak of the FT gives the number of oxygen atoms belonging to the carboxylate groups.

When the dimeric complex is considered, the main features remain (solid line in Figures 4A-B). The difference is mainly explained by the contribution resulting from the single scattering on Eu backscatterer (scattering path 8 in Table 2). This leads to higher amplitudes of the EXAFS oscillations for k values above 10 $Å^{-1}$ resulting in a higher contribution in the third peak of the FT. This Eu-Eu contribution is however less important considering the k range explored in this study (Figure 5B, dotted line) (k range =1.5-11.5 $Å^{-1}$).

From a quantitative point of view, the description of the EXAFS spectra appears difficult. 155 and 202 scattering paths (considering a cluster radius of 5 Å) are needed to reconstruct the spectra for monomer and dimer complex, respectively. This can be simplified using only the main contributions with a scattering contribution above 10%. However, the number of contributions remains still too important for a fitting (34 and 27 for dimer and monomer complexes, respectively). The high number of contributions to consider results from the distorded structure of the clusters: based on the crystal structure with the space group $P\bar{1}$ [29.], each Eu-O bonding has a different bond length.

A further simplification would be to consider only one type of water molecule and carboxylate group, i.e a mean distance is taken for Eu-$O(H_2)$, Eu-O(Ac), Eu-C(1,3,5) and Eu-C(1,3,5)-C(2,4,6) contributions (see Table 2). In that case, O9 from the bridge (Figure 1) is associated to one oxygen atom from a water molecule. The consideration of only one oxygen shell without distinction between coordination water molecules and carboxylate groups was also considered. This simplification leads to a significant overestimation of the numer of oxygen atoms after reconstruction of EXAFS spectrum. In conclusion, eight scattering contributions are considered (see Table 2). The results correspond to the dotted line in Figures

4C-D for the dimer complex. This simplification is not sufficient to reconstruct the theoretical spectra precisely, and therefore it may lead to errors in the fitted parameters in case of a distored structure.

Reference compound: The measured EXAFS spectrum of $Eu(Ac)_3 \cdot xH_2O$ is given in Figure 6A together with its Fourier transform (Figure 6B). As expected, the FT presents two main peaks at R+ΔR values of 1.9 and 3.9 Å. The spectrum was fitted to the EXAFS equation considering the 8 scattering contributions given in Table 2. The results, given in Table 2, are in agreement with the structural parameters of the reference compound given in the literature [29]:

- The second peak is the result of the contribution of scattering paths 5-7 in agreement with the bidendate mode of coordination characterized by IR. A Eu-Eu contribution needs also to be considered for a good fitting. The number of Eu in the shell was fixed to one in the fittings.
- The first peak is the contribution of scattering paths 1-3. 3.4±0.7 coordination water molecules and 2.3±0.5 carboxylate groups coordinated to Eu were obtained by the fitting procedure. The total coordination number around Eu (7.9±1.6) corresponds within experimental errors to the crystal structure. The number of carboxylate groups coordinated however appears slightly underestimated. This may be the consequence of the contribution of the impurity revealed by LIFS (1:2 Eu:Ac complex) and/or of the distored structure as discussed before. Concerning the distances obtained, they agree with those expected.

Finally, one can conclude that the simplification for the cluster description appears acceptable.

EuPAA complex: The measured EXAFS spectrum is given in Figure 6C together with its Fourier transform (Figure 6D). The typical multiple scattering spectral features of a bidendate coordination mode is not present. On the other hand, two small peaks can be observed at R+ΔR values of 2.6 and 3.5 Å. The first assumption is to consider that there is a monodendate mode of coordination between Eu and acetate groups (case 1). Another possibility is to consider a constrained bidendate mode of coordination (case 2), i.e. Eu and carbon atoms are not exactly on the same line (no foccusing effect). This could be explained by a low degree of freedom of PAA carboxylate groups: the methylene chains of PAA are flexible enough to allow two acetate groups to approach each other to form the complex but within a more sterically constrained cage-like environment than for 1:2 Eu:Ac complex. Both assumptions were tested.

In the first case, in addition to scattering paths 1-2, the scattering of the photoelectron by carbon atoms was also considered. The monodendate coordination was modeled by the sequence Eu(1)-O(9)-C(5b) (Figure 1). Based on the theoretical calculation made with the dimer, in addition to the SS paths, the 2 degenerated 3-legged and 4-legged MS paths were considered (see Table 2, scattering paths 9-11). For the second case, scattering paths 1-4 were taken into account. For scattering path 4, a mean value was considered in the fitting.

The results are presented in Figure 6C-D as dotted lines. No significant difference is observed between both models. The total coordination number appears identical in both cases (7.7). The complexed species are $EuAc_{2.3}.5.4H_20$ and $EuAc_{1.3}.5.2H_20$ for case 1 and 2, respectively. Concerning the distances, they agree with what was measured for the reference compound in case 2, whereas in case 1, the distance is either higher ($O(H_2)$; 2.45 Å) or lower (O(Ac); 2.31 Å) than that expected (2.39 Å). Considering the possible distored structure of the Eu environment, none of these results allows to discrime between both assumptions. On the other hand, results obtained by IR and LIFS would suggest case 2 as more reliable.

$EuPAA_{ads}$ complex: The EXAFS spectrum and its Fourier transform are presented in Figure 6E-F. One can observe the spectral characteristics of the multiple scattering paths related with a bidendate mode of coordination. The parameters obtained from the fitting are given in Table 2. The peak at R+ΔR = 3.9Å can be completely reproduced by the multiple scattering paths 5-7. No Eu-Eu interaction needs to be considered in the fit, although its presence cannot be excluded because its scattering contribution is weak in the explored k range (see reference compound and theoretical considerations). In agreement with LIFS results, two carboxylate groups bound to Eu are deduced from the fitting procedure. To complete the oxygen scattering path, 2-3 oxygen atoms are needed at a distance of 2.32 Å. They probably belong to the coordination water molecules. It must be noticed that the total coordination number obtained (7.1±1.4) appears lower than those deduced from reference (7.9±1.6) and $EuPAA_{ads}$ (7.7±1.6) complexes. This may suggest a diminution of the total coordination number in the ternary system.

Summary

The spectroscopic techniques used in this study show the formation of slightly different species in EuPAA and $EuPAA_{ads}$ complexes. Two carboxylate groups with 2-3 (ternary system) and 4-5 (binary system) water molecules are coordinated to Eu in the first coordination sphere. For $EuPAA_{ads}$ complex, the coordination mode between carboxylate groups and Eu appears to be bidendate, as observed for crystalline $Eu(Ac)_3 \cdot xH_2O$. A similar mode of coordination is probable for EuPAA complex but with a sligthy distored coordination, i.e. Eu, C(1,3,5) and C(2,4,6) atoms are not on the same plan. It can be concluded that the degree of freedom of carboxylate groups is not the same for free or adsorbed PAA. For PAA, the freedom is constrained by the flexibility of the methylene chain.

For PAA_{ads}, the polymer chains cannot any more be treated as independent chains. The results of this investigation support our previous assumption [18] of aggregates that form an organic layer at the mineral surface which can be viewed as a gel-like structure with a high concentration of carboxylate groups.

Acknowledgements

The work is included in the EC Nework Of Excellence Actinet (PAA project 02-15). The money given for mobility measures is gratefully acknowledged. The authors are grateful to Pr. E. Simoni and G. Lagarde (Institut de Physique Nucléaire, Orsay) to allow us to use the apparatus of LIFS. We are grateful to ESRF for the beam time allocation and to Dr A. Rossberg at ROBL for his help in measuring the spectra.

References

1. G.R. Choppin, In Chemical Separation Technologies and Related Methods of Nuclear Waste Management, Kluwer Academic Publ., Dordrecht, 1999.
2. K. Czerwinski, J.I. Kim, Mater. Res. Soc. Proc. 465 (1997) 743.
3. W. Hummel, In Modelling in Aquatic Chemistry, OECD Nuclear Energy Agency, Paris, 1997.
4. M.A. Glaus, W. Hummel, L.R. Van Loon, Appl. Geochem. 15 (2000) 943.
5. M. Samadfam, S. Sato, H. Ohashi, Radiochim. Acta 82 (1998) 361.
6. Th. Rabung, H. Geckeis, J.I. Kim, H.P. Beck, Radiochim. Acta 82 (1998) 82.
7. A.J. Fairhurst, P. Warwick, S. Richardson, Colloids Surfaces A: Physicochem. Eng. Aspects 99 (1995) 187.
8. B. Allard, V. Moulin, L. Basso, M.T. Tran, D. Stammose, Geoderma 44 (1989) 181.
9. C.H. Ho, N.H. Miller, J. Colloid Interf. Sci. 106 (1985) 281.
10. L. Righetto, G. Bidoglio, G. Azimonti, I.R. Bellodono, Environ. Sci. Technol. 25 (1991) 25.
11. J.J. Lenhart, B.D. Honeyman, Geochim. Cosmochim. Acta. 63 (1999) 2891.
12. P. Reiller, V. Moulin, F. Casanova, C. Dautel, Appl. Geochem. 17 (2002) 1551.
13. N. Labonne-Wall, V. Moulin, J-P. Vilarem, Radiochim. Acta 79 (1997) 37.
14. A.W.P. Wermeer, J.K. Mcculloch, W.H. Van Riemsdijk, L.K. Koopal, Environ. Sci. Technol. 33 (1999) 3892.
15. Y. Takahashi, T. Kimura, Y. Kato, Y. Minai, Environ. Sci. Technol. 33 (1999) 4016.
16. R.M. Floroiu, A.P. Davis, A. Torrents, Environ. Sci. Technol. 35 (2001) 348.
17. G. Montavon, S. Markai, Y. Andrès, B. Grambow, Environ. Sci. Technol. 36 (2002) 3303.

18. G. Montavon, T. Rabung, H. Geckeis, B. Grambow, Environ. Sci. Technol. 38 (2004) 4312.
19. G. Montavon, B. Grambow, New J. Chem. 27 (2003) 1344.
20. F.S. Richardson, Chem. Rev. 82 (1982) 541.
21. G.R. Choppin, Z.M. Wang, Inorg. Chem. 36 (1997), 249.
22. T. Rabung, T. Stumpf, H. Geckeis, R. Klenze, J.I. Kim, Radiochim. Acta 88 (2000) 711.
23. G. Montavon, S. Markai, B. Grambow, Radiochim. Acta 90 (2002) 689.
24. E. Ordoñez-Regil, R. Drot, E. Simoni, and J. J. Ehrhardt, Langmuir 18 (2002) 7977.
25. C.W. MaNemar, W. D. Horrocks Jr., Appl. Spectrosc. 43 (1989) 816.
26. W. Matz, N. Schell, G. Bernhard, F. Prokert, T. Reich, J. Claußner, W. Oehme, R. Schlenk, S. Dienel, H. Funke, F. Eichhorn, M. Betzl, D. Pröhl, U. Strauch, G. Hüttig, H. Krug, W. Neumann, V. Brendler, P. Reichel, M.A. Denecke, H. Nitsche, J. Synchrotron Rad. 6 (1999) 1076.
27. G.N. Geoge, I.J. Pickering, EXAFSPAK: A suite of computer programs for analysis of x-ray absorption spectra, Stanford Synchrotron Radiation Laboratory, Stanford, CA, USA 1995.
28. A.L. Ankudinov, B. Ravel, J.J. Rehr, S.D. Conradson: Multiple-scattering calculations of x-ray-absorption spectra, Phys. Rev. B. 52 (1998) 7565.
29. Y. Yansheng, L. Lubin, J. Struct. Chem. 7 (1988) 1.
30. B.Ravel, J. Synchrotron Rad. 8 (2001) 314.
31. T.H. Yoon, H. Moon, Y.J. Park, K.K. Park, Environ. Sci. Technol. 28 (1994) 2139.
32. G.B. Deacon and R.J. Phillips, Coord. Chem. Rev, 33 (1980) 227.
33. W. D. Horrocks Jr., D.R. Sudnick, J. Am. Chem. Soc. 101 (1979) 334.
34. R.M. Smith, A.E. Martell, In critical stability constants, Vol3: other organic ligands, Plenum press, New York and London (1989).

Table 1 LIFS results.

	Conditions			EXCITATION SPECTRA						Remark
				I1 (%)	W1	L1	I2 (%)	W2	L2	
REFERENCE	[Eu]=10^{-3}M, [Ac]=4.5.10^{-3}M, pH=6	Eu + 1:1 complex *	sol.	28±2	578.80± 0.01	0.52±0.02	72±2	578.99± 0.01	0.20±0.01	_
	[Eu]=10^{-3}M, [Ac]=0.3M, pH=6	1:2 + 1:3 complexes *	sol.	96±3	579.18± 0.02	0.38±0.01	4±2	579.53± 0.04	0.3 (f)	
	$Eu(Ac)_3.xH_20$	_	h.s.	23±3	579.21± 0.02	0.16±0.03	67±2	579.67± 0.01	0.22±0.01	used for EXAFS
EuPAA	[Eu]=10^{-4}M, (PAA)=0.83g/L	r=12	h.s.	14±13	578.8±0 .4	0.72±0.08	86±22	579.22± 0.02	0.46±0.05	used for EXAFS
$EuPAA_{ads}$	c=0.5g/L, [Eu]=1.10^{-7}M	r=3330	h.s.	100	579.22± 0.01	0.49±0.01	_	_	_	
	c=5g/L, [Eu]=1.10^{-5}M	r=334	h.s.	_	_	_	_	_	_	
	c=5g/L, [Eu]=1.10^{-4}M	r=34	h.s.	17±2	578.78± 0.08	0.86±0.06	83±3	579.22 (f)	0.49 (f)	used for EXAFS
	c=0.5g/L, [Eu]=1.10^{-5}M	r=34	sus.	100	579.17 ±0.01	0.41±0.0 1	_	_	_	
	c=0.5g/L, [Eu]=1.10^{-6}M	r=333	sus.							
	c=5g/L, [Eu]=1.10^{-6}M	r=3330	sus.							

legend: (f): parameter fixed for the fitting; h.s.: hydrated solid; sus.: suspension; sol.: solution. * Composition deduced from calculation made with the constants given in [34].

Table 2. Results of EXAFS spectra analysis. Scattering paths (SP) 2-7 and 9-11 are related to bidentate and monodendate coordination modes, respectively. Parameters in bold are linked.

●: Eu; ●:C; ●: O.

			DIMER, theoretical considerations	Reference coupound	EuPAA		EuPAA$_{ads}$
					case 1	case 2	
SP 1	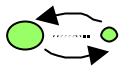	N	3 (f)	3.4	5.4	5.2	2.5
		R (Å)	2.39 (f)	2.36	2.45	2.38	2.32
		s^2 (Å^2)	–	0.0035	0.0054	0.0069	0.0032
		DE_0		-10.9 [a]	-10.5 [a]	-9.7 [a]	-10.9 [a]
SP 2		N	6 (f)	4.5 [b]	1.6 [b]	2.6 [b]	4.6 [b]
		R (Å)	2.49 (f)	2.49	2.31	2.52	2.44
		s^2 (Å^2)	–	0.0032	0.002	0.0043	0.0032
		DE_0		**-10.9 [a]**	**-10.5 [a]**	**-9.7 [a]**	**-10.9 [a]**
SP 3	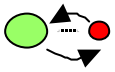	N	3 (f)	**2.25 [b]**	–	**1.3 [b]**	**2.3 [b]**
		R (Å)	2.87 (f)	2.89		2.88	2.99
		s^2 (Å^2)	–	0.0071		0.004	0.0053
		DE_0		**-10.9 [a]**		**-9.7 [a]**	**-10.9 [a]**
SP 4	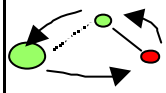	N	12 (f)	**9 [b]**	–	**5.2 [b]**	**9.2 [b]**
		R (Å)	3.31 (f)	3.26		3.31	3.37
		s^2 (Å^2)	–	0.019		0.003	0.0065
		DE_0		**-10.9 [a]**		**-9.7 [a]**	**-10.9 [a]**
SP 5	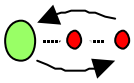	N	3 (f)	**2.25 [b]**	–		**2.3 [b]**
		R (Å)	4.37 (f)	4.37 [c]			4.41 [c]
		s^2 (Å^2)	–	0.0035 [d]			0.0023 [d]
		DE_0		**-10.9 [a]**			**-10.9 [a]**
SP 6	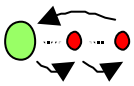	N	6 (f)	**4.5 [b]**	–		**4.6 [b]**
		R (Å)	4.37 (f)	**4.37 [c]**			**4.41 [c]**
		s^2 (Å^2)	–	**0.0035 [d]**			**0.0023 [d]**
		DE_0		**-10.9 [a]**			**-10.9 [a]**
SP 7	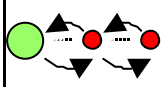	N	3 (f)	**2.25 [b]**	–		**2.3 [b]**
		R (Å)	4.37 (f)	**4.37 [c]**			**4.41 [c]**
		s^2 (Å^2)	–	**0.0035 [d]**			**0.0023 [d]**
		DE_0		**-10.9 [a]**			**-10.9 [a]**
SP 8	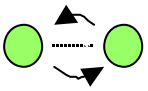	N	1 (f)	1 (f)	–		–
		R (Å)	4.22 (f)	4.18			
		s^2 (Å^2)	–	0.01			
		DE_0		**-10.9 [a]**			
SP 9		N	–	–	**1.6 [b]**	–	–
		R (Å)			3.47 [c]		
		s^2 (Å^2)			0.009 [d]		
		DE_0			**-10.5 [a]**		
SP 10	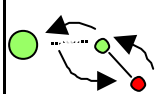	N	–	–	**3.2 [b]**	–	–
		R (Å)			**3.47 [c]**		
		s^2 (Å^2)			**0.009 [d]**		
		DE_0			**-10.5 [a]**		
SP 11	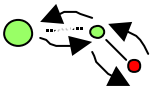	N	–	–	**1.6 [b]**	–	–
		R (Å)			**3.47 [c]**		
		s^2 (Å^2)			**0.009 [d]**		
		DE_0			**-10.5 [a]**		

parameters; the letter gives the link. (f): fixed parameter in the fitting procedure.

Figure captions.

Figure 1: Representation of the dimeric coumpound of europium triacetate [29].

Figure 2: Excitation spectra measured for the reference system (see Table 1; A: Eu + 1:1 complex; B: 1:1 + 1:2 complex; C: $EuAc_3.xH_2O$). The lines represent the fittings done with the parameters given in Table 1.

Figure 3: Excitation spectra measured in the binary (b.s.) and ternary (t.s.) systems with hydrated solids (h.s.) or suspensions (sus.) (see Table 1). The lines represent the fittings done with the parameters given in Table 1.

Figure 4: Infrared spectra of $EuAc_3$ and EuPAA complexes.

Figure 5: EXAFS spectra and their corresponding Fourrier tranforms. (A-B) theoretical results for dimer and monomer complexes. (C-D) I: theoretical spectrum; II: spectrum recalculated considering simplifications (see text and Table 1).

Figure 6: EXAFS spectra and their corresponding FT's for reference $Eu(Ac)_3 \cdot xH_2O$, EuPAA and $EuPAA_{ads}$ complexes. Comparison between experiment and calculation. The parameters used for the calculation are given in Table 2.

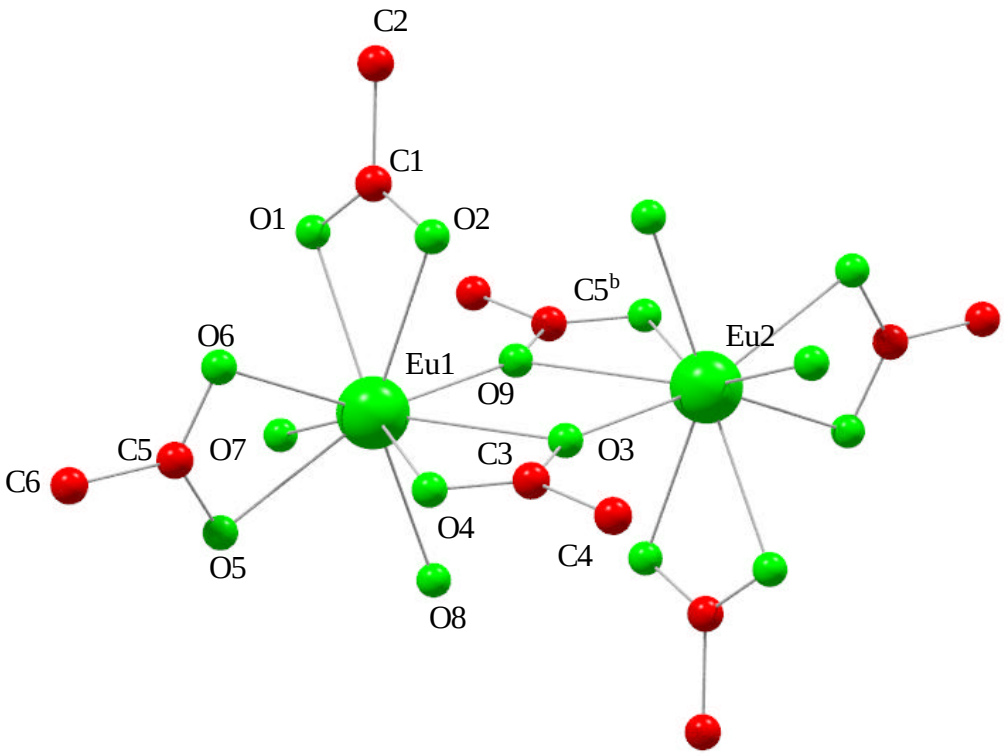

Figure 1

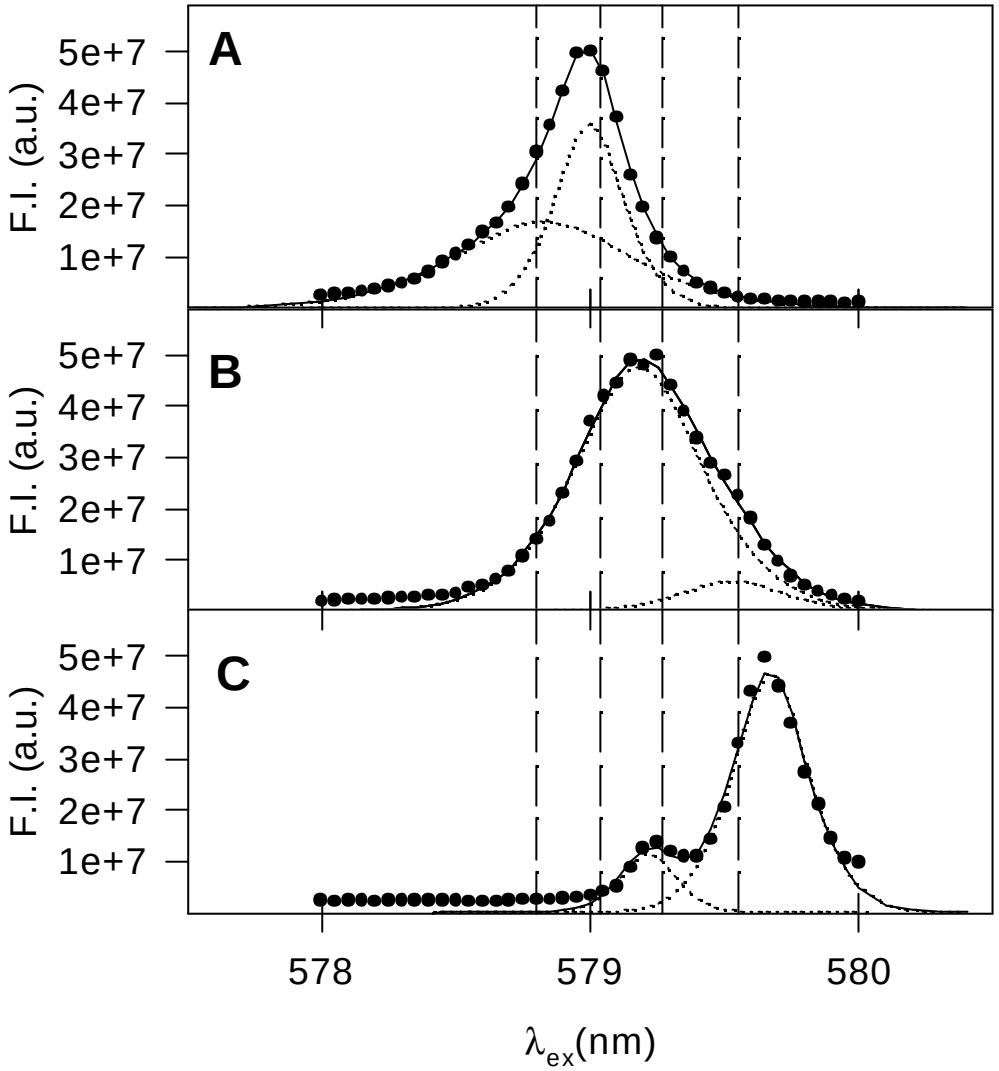

Figure 2

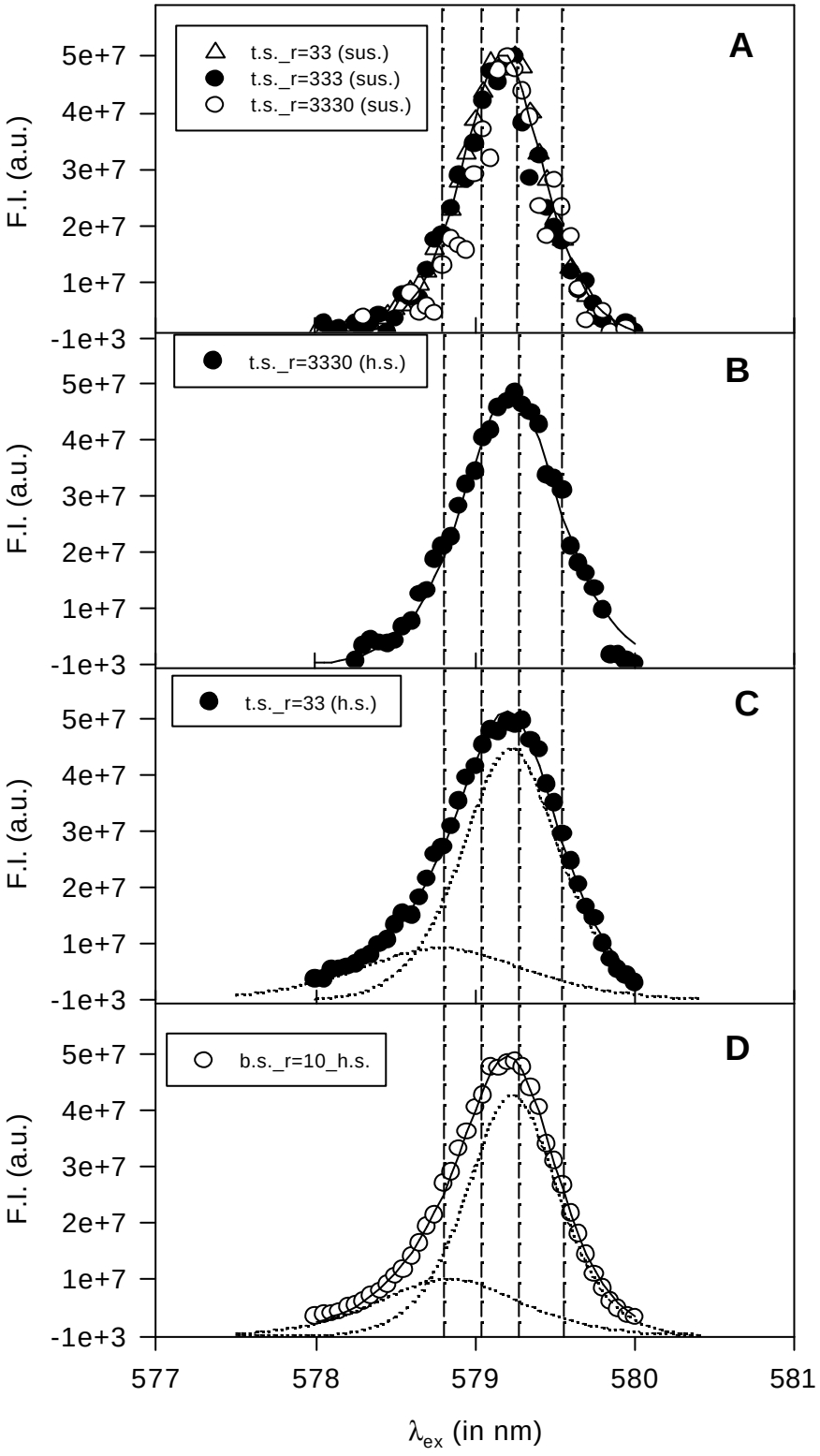
A
t.s._r=33 (sus.)
t.s._r=333 (sus.)
t.s._r=3330 (sus.)
B
t.s._r=3330 (h.s.)
C
t.s._r=33 (h.s.)
D
b.s._r=10_h.s.
F.I. (a.u.)
5e+7
4e+7
3e+7
2e+7
1e+7
-1e+3
577
578
579
580
581
λex (in nm)

Figure 3

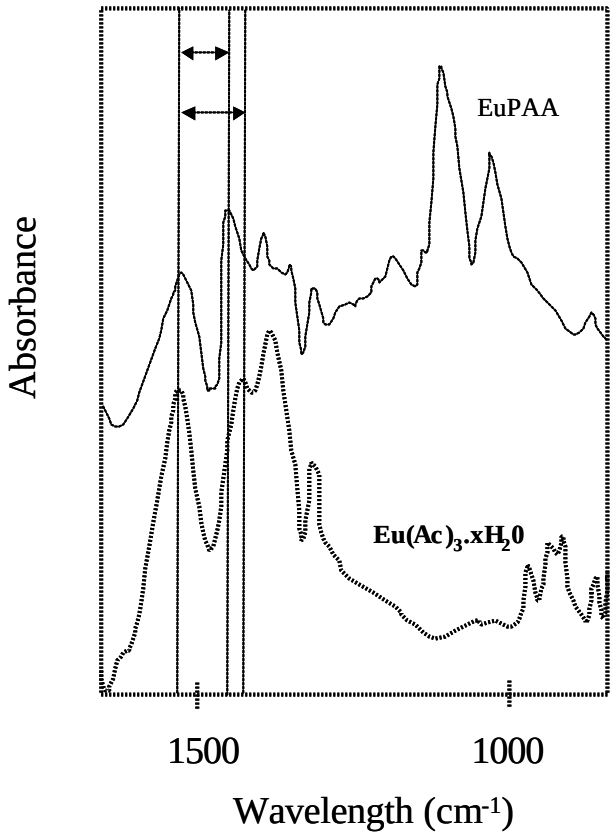

Figure 4

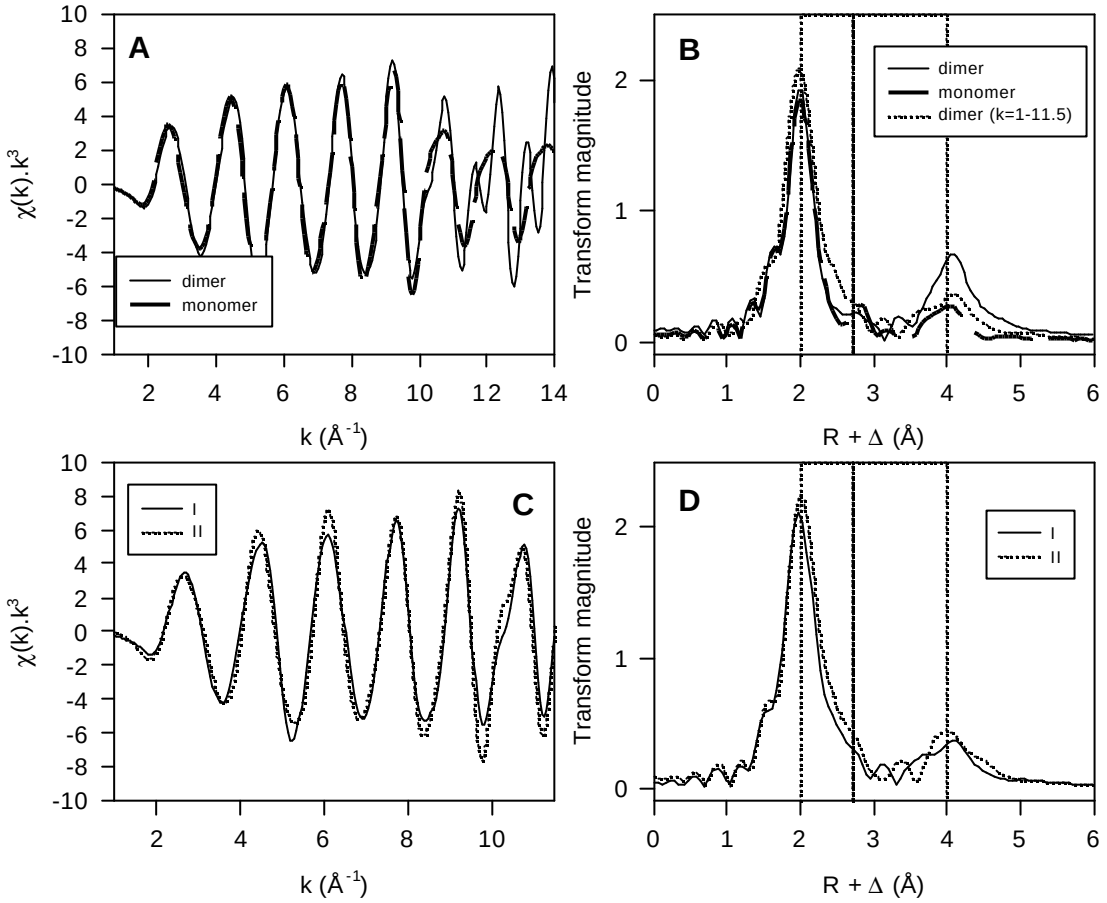
A
B
C
D
dimer
monomer
dimer (k=1-11.5)
I
II
χ(k).k³
k (Å⁻¹)
Transform magnitude
R + Δ (Å)

Figure 5

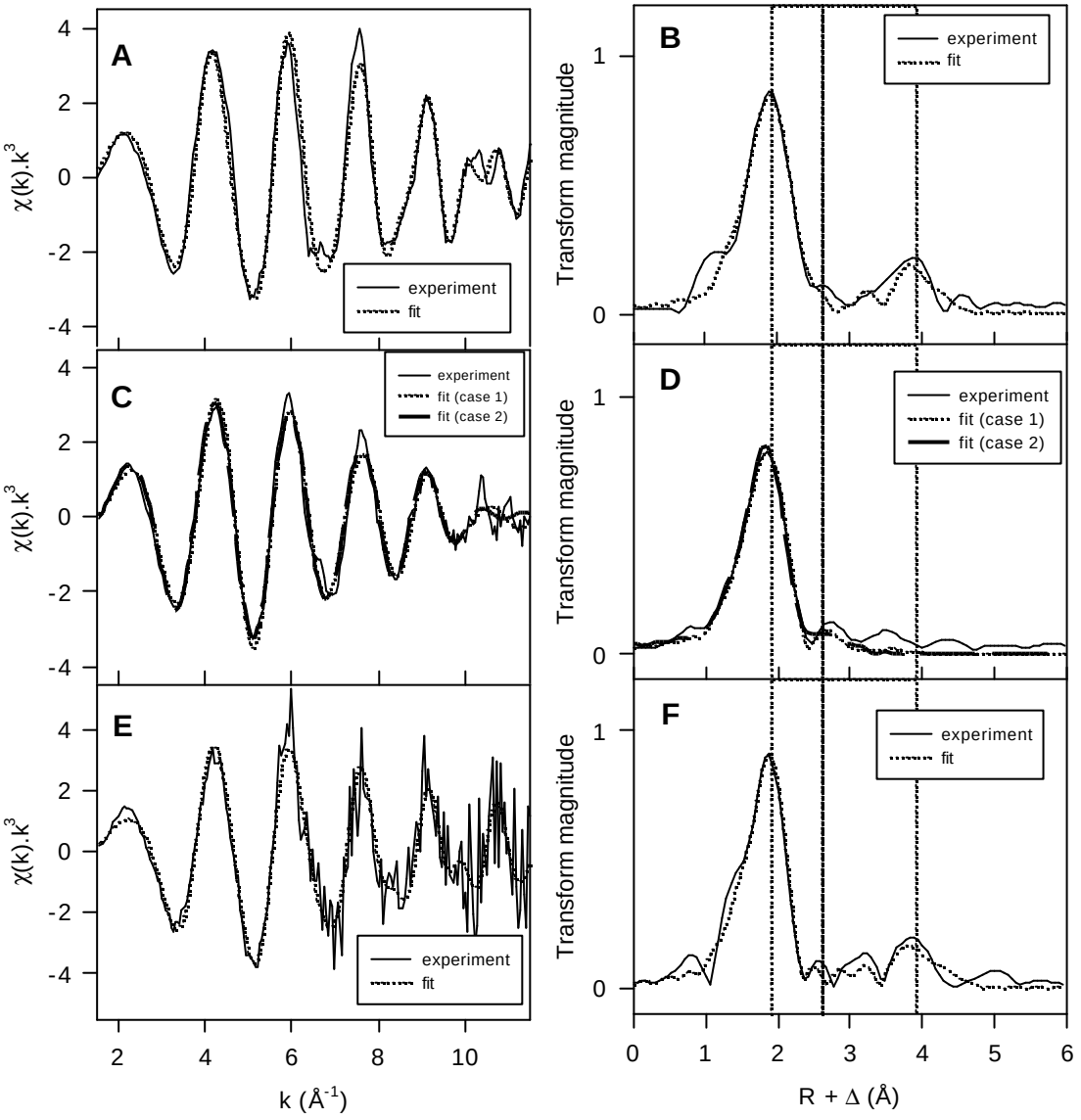
A
B
C
D
E
F
experiment
fit
fit (case 1)
fit (case 2)
χ(k).k3
Transform magnitude
k (Å-1)
R + Δ (Å)

Figure 6